

# Facile collection of two-dimensional electronic spectra using femtosecond pulse-shaping technology

Erik M. Grumstrup,<sup>1,‡</sup> Sang-Hee Shim,<sup>2,‡</sup> Matthew A. Montgomery,<sup>1,‡</sup>  
Niels H. Damrauer,<sup>1,\*</sup> and Martin T. Zanni<sup>2,\*</sup>

<sup>1</sup> Department of Chemistry and Biochemistry, University of Colorado, Boulder, Colorado 80309-0215, USA

<sup>2</sup> Department of Chemistry, University of Wisconsin-Madison, Madison, WI 53706-1396, USA

<sup>‡</sup>Each of these authors made essential contributions to the research

\*Corresponding authors: [niels.damrauer@colorado.edu](mailto:niels.damrauer@colorado.edu) and [zanni@chem.wisc.edu](mailto:zanni@chem.wisc.edu)

**Abstract:** This letter reports a straightforward means of collecting two-dimensional electronic (2D-E) spectra using optical tools common to many research groups involved in ultrafast spectroscopy and quantum control. In our method a femtosecond pulse shaper is used to generate a pair of phase stable collinear laser pulses which are then incident on a gas or liquid sample. The pulse pair is followed by an ultrashort probe pulse that is spectrally resolved. The delay between the collinear pulses is incremented using phase and amplitude shaping and a 2D-E spectrum is generated following Fourier transformation. The partially collinear beam geometry results in perfectly phased absorptive spectra without phase twist. Our approach is much simpler to implement than standard non-collinear beam geometries, which are challenging to phase stabilize and require complicated calibrations. Using pulse shaping, many new experiments are now also possible in both 2D-E spectroscopy and coherent control.

©2007 Optical Society of America

**OCIS codes:** (300.6530) Ultrafast Spectroscopy; (300.0550) Visible Spectroscopy; (320.5540) Pulse Shaping.

---

## References and links

1. "Special Issue on Multidimensional Spectroscopies," *Chem. Phys.* **266**, 135-352 (2001).
2. "Multidimensional Ultrafast Spectroscopy Special Feature," *Proc. Natl. Acad. Sci. USA* **104**, 14189-14544 (2007).
3. F. Ding, P. Mukherjee, and M. T. Zanni, "Passively correcting phase drift in two-dimensional infrared spectroscopy," *Opt. Lett.* **31**, 2918-2920 (2006).
4. G. D. Goodno, G. Dadusc, and R. J. D. Miller, "Ultrafast heterodyne-detected transient-grating spectroscopy using diffractive optics," *J. Opt. Soc. Am. B* **15**, 1791-1794 (1998).
5. T. Brixner, T. Mancal, I. V. Stiopkin, and G. R. Fleming, "Phase-stabilized two-dimensional electronic spectroscopy," *J. Chem. Phys.* **121**, 4221-4236 (2004).
6. V. Volkov, R. Schanz, and P. Hamm, "Active phase stabilization in Fourier-transform two-dimensional infrared spectroscopy," *Opt. Lett.* **30**, 2010-2012 (2005).
7. T. H. Zhang, C. N. Borca, X. Q. Li, and S. T. Cundiff, "Optical two-dimensional Fourier transform spectroscopy with active interferometric stabilization," *Opt. Express* **13**, 7432-7441 (2005).
8. H. Kawashima, M. M. Wefers, and K. A. Nelson, "Femtosecond Pulse Shaping, Multiple-Pulse Spectroscopy, and Optical Control," *Annu. Rev. Phys. Chem.* **46**, 627-656 (1995).
9. M. A. Dugan, J. X. Tull, and W. S. Warren, "High-resolution acousto-optic shaping of unamplified and amplified femtosecond laser pulses," *J. Opt. Soc. Am. B* **14**, 2348-2358 (1997).
10. T. Weinacht, J. Ahn, and P. Bucksbaum, "Controlling the shape of a quantum wavefunction," *Nature* **397**, 233-235 (1999).
11. T. C. Weinacht, J. Ahn, and P. H. Bucksbaum, "Measurement of the amplitude and phase of a sculpted Rydberg wave packet," *Phys. Rev. Lett.* **80**, 5508-5511 (1998).

12. J. B. Asbury, T. Steinel, and M. D. Fayer, "Vibrational echo correlation spectroscopy probes of hydrogen bond dynamics in water and methanol," *J. Lumin.* **107**, 271-286 (2004).
13. E. B. W. Lerch, X. C. Dai, S. Gilb, E. A. Torres, and S. R. Leone, "Control of  $\text{Li}_2$  wave packet dynamics by modification of the quantum mechanical amplitude of a single state," *J. Chem. Phys.* **124** (2006).
14. P. F. Tian, D. Keusters, Y. Suzuki, and W. S. Warren, "Femtosecond phase-coherent two-dimensional spectroscopy," *Science* **300**, 1553-1555 (2003).
15. J. C. Vaughan, T. Hornung, K. W. Stone, and K. A. Nelson, "Coherently controlled ultrafast four-wave mixing spectroscopy," *J. Phys. Chem. A* **111**, 4873-4883 (2007).
16. S.-H. Shim, D. B. Strasfeld, Y. L. Ling, and M. T. Zanni, "Automated 2D IR spectroscopy using a mid-IR pulse shaper and application of this technology to the human islet amyloid polypeptide," *Proc. Natl. Acad. Sci. USA* **104**, 14197-14202 (2007).
17. S. M. G. Faeder, and D. M. Jonas, "Two-dimensional electronic correlation and relaxation spectra: Theory and model calculations," *J. Phys. Chem. A* **103**, 10489-10505 (1999).
18. M. Khalil, and A. Tokmakoff, "Signatures of vibrational interactions in coherent two-dimensional infrared spectroscopy," *Chem. Phys.* **266**, 213-230 (2001).
19. C. Scheurer and S. Mukamel, "Design strategies for pulse sequences in multidimensional optical spectroscopies," *J. Chem. Phys.* **115**, 4989-5004 (2001).
20. M. A. Montgomery, R. R. Meglen, and N. H. Damrauer, "General method for the dimension reduction of adaptive control experiments," *J. Phys. Chem. A* **110**, 6391-6394 (2006).
21. P. F. Tekavec, G. A. Lott, and A. H. Marcus, "Flourescence-Detected Two-Dimensional Electronic Coherence Spectroscopy by Acousto-Optic Phase Modulation," *J. Chem. Phys.*, Submitted (2007).
22. S. Mukamel, *Principles of Nonlinear Optical Spectroscopy* (Oxford University Press, New York, 1995).
23. E. C. Fulmer, F. Ding, P. Mukherjee, and M. T. Zanni, "Vibrational dynamics of ions in glass from fifth-order two-dimensional infrared spectroscopy," *Phys. Rev. Lett.* **94**, 067402 (2005).
24. E. C. Fulmer, P. Mukherjee, A. T. Krummel, and M. T. Zanni, "A pulse sequence for directly measuring the anharmonicities of coupled vibrations: Two-quantum two-dimensional infrared spectroscopy," *J. Chem. Phys.* **120**, 8067-8078 (2004).
25. W. M. Zhang, V. Chernyak, and S. Mukamel, "Multidimensional femtosecond correlation spectroscopies of electronic and vibrational excitons," *J. Chem. Phys.* **110**, 5011-5028 (1999).
26. D. Keusters, H. S. Tan, and W. S. Warren, "Role of pulse phase and direction in two-dimensional optical spectroscopy," *J. Phys. Chem. A* **103**, 10369-10380 (1999).
27. J. C. Vaughan, T. Feurer, K. W. Stone, and K. A. Nelson, "Analysis of replica pulses in femtosecond pulse shaping with pixelated devices," *Opt. Express* **14**, 1314-1328 (2006).
28. R. Trebino, *Frequency-Resolved Optical Gating* (Kluwer Academic Publishers, Norwell, MA, 2000).
29. R. S. Judson and H. Rabitz, "Teaching lasers to control molecules," *Phys. Rev. Lett.* **68**, 1500-1503 (1992).
30. S. A. Rice and M. Zhao, *Optical Control of Molecular Dynamics*. (Wiley, New York, 2000).
31. M. A. Montgomery, and N. H. Damrauer, "Elucidation of control mechanisms discovered during adaptive manipulation of  $[\text{Ru}(\text{dpp})_3](\text{PF}_6)_2$  emission in the solution phase," *J. Phys. Chem. A* **111**, 1426-1433 (2007).
32. M. A. Montgomery, R. R. Meglen, and N. H. Damrauer, "General method for reducing adaptive laser pulse-shaping experiments to a single control variable," *J. Phys. Chem. A* **111**, 5126-5129 (2007).
33. T. Brixner, N. H. Damrauer, B. Kiefer, and G. Gerber, "Liquid-phase adaptive femtosecond quantum control: Removing intrinsic intensity dependencies," *J. Chem. Phys.* **118**, 3692-3701 (2003).
34. T. Brixner, N. H. Damrauer, and G. Gerber, "Femtosecond quantum control," in *Advances in Atomic, Molecular, and Optical Physics, Vol 46*(2001), pp. 1-54.

## 1. Introduction

Multidimensional electronic and infrared spectroscopies are two powerful classes of techniques used to study fundamental problems in chemistry, biology and physics. By correlating electronic or vibrational transition dipoles in two- or three-dimensions, these methods provide information on molecular structure, coupling between oscillators, and energy transfer. They have been exploited to study protein structure and folding, liquid dynamics, energy transfer in photosynthetic proteins, and carrier dynamics in semiconductors, to name just a few experiments [1, 2].

The most common applications of multidimensional infrared and electronic spectroscopies are two-dimensional versions, called 2D-IR or 2D-E, respectively. While interpretation of the 2D spectra depends on the application, the two techniques use virtually identical sequences of femtosecond pulses and both transform the data in the same way. Figures 1(a) and 1(b) show two beam geometries that have been used previously to collect 2D spectra. The 2D data sets are collected as a function of the time between the first two pulses ( $t_1$ ) and last two pulses ( $t_3$ ) and Fourier transformed to the frequency domain. Alternatively, the  $t_3$  delay can be collected directly in the frequency domain using a spectrometer, as we do here. The only significant difference between the infrared and visible versions is the wavelength of light. However,

because these techniques require interferometric phase stability, this seemingly small difference has led to dramatically different approaches in their implementation. High phase stability is relatively easy to achieve in the infrared where the long wavelengths give rise to slow phase drift that can be corrected in a straightforward manner [3]. On the other hand, achieving adequate phase stability with visible laser pulses can be difficult. In most 2D spectrometers, each of the four pulses traverse an independent delay line whose length must not vary more than a fraction of the wavelength during the experiment. One approach for stabilizing the pathlengths is to use diffractive optics and phase-compensating mirror arrangements [4, 5]. Another is to actively adjust the optical pathlengths using piezocrystals and two sets of HeNe interferometers for feedback [6, 7]. Either approach results in high quality multidimensional electronic spectra, but the extensive infrastructure and effort required to implement these methods has discouraged all but a few dedicated groups from using this extremely powerful research tool. In this paper, we report a method that significantly eases the hurdles associated with collecting 2D electronic spectra. We show that 2D-E spectra can be measured using commonly available pulse shapers and a partially collinear pump-probe beam geometry. With a pulse shaper it is a trivial matter to make phase stable pulse trains [8-11], thus eliminating difficulties associated with working at short (visible) wavelengths. Furthermore, the beam geometry used in our experiments eliminates the need for complicated phasing procedures [5, 12]. Our method eliminates many of the technical hurdles to implementing 2D-E spectroscopy, making it possible for many more research groups to exploit this powerful spectroscopy in their research.

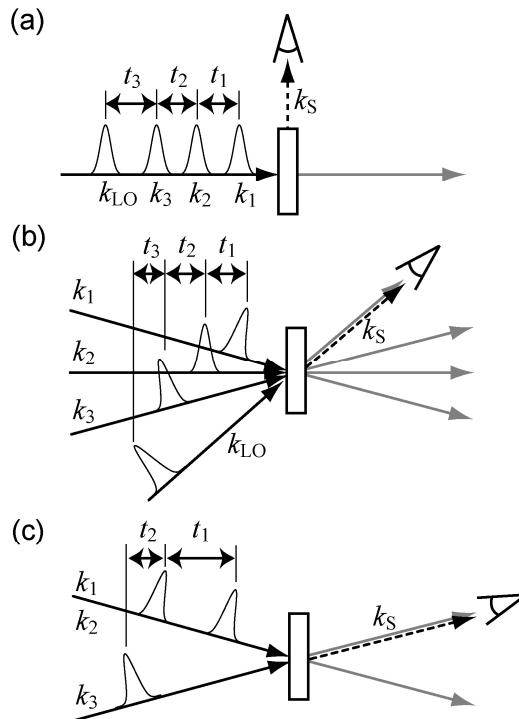


Fig. 1. Methods for collecting 2D spectra.  $k_n$  are the wavevectors (directions) of the excitation pulses and  $k_s$  is the wavevector of the emitted signal. (a) An entirely collinear pulse sequence in which fluorescence is collected orthogonally to the beam path. (b) A boxcar type of geometry in which all four beams propagate at different angles. (c) The partially collinear geometry employed here in which two “pump” pulses are followed by an off axis “probe” pulse which is then spectrally resolved.

It is straightforward to generate phase-locked pulse pairs with a pulse shaper capable of modulating the spectrum of femtosecond pulses [8-11, 13]. Warren and coworkers used this fact to generate an entirely collinear train of 4 pulses (Fig. 1(a)) [9]. Using this pulse train, they were able to collect 2D-E spectra in analogy to the way that 2D NMR spectra are generated using phase cycling [14]. However, the fully collinear geometry necessitates the signal be measured by some observable other than absorption (e.g. fluorescence), since the intense excitation pulses will saturate the detector in a linear absorption arrangement. In contrast, Nelson and coworkers used a two-dimensional pulse shaper to collect 2D-E spectra in a non-collinear boxcar geometry where all 4 pulses in the pulse train impinge on the sample from different directions [15], similar to the geometry of traditional 2D spectroscopies (Fig. 1(b)). The approach by Nelson and coworkers takes advantage of phase matching that provides background free signal and eliminates the need for phase cycling. However, the two-dimensional pulse shaper is not widely available and has very low throughput efficiency owing to the fact that the input laser beam is spatially filtered to obtain the non-collinear geometry.

Our method of collecting 2D-E spectra mirrors recent work using a mid-IR pulse shaper to collect 2D IR spectra [16]. Our approach uses a “pump/probe” beam geometry [17, 18] where the collinear pulse pair “pump” is generated by a pulse shaper (Fig. 1(c)). This partially collinear beam geometry coupled with a pulse shaper retains the strengths of the Warren and Nelson approaches, but automatically generates perfectly phased spectra at the highest-resolution possible. Fluorescence detection is not necessary, which widens the range of samples that can be studied and phase cycling, while not necessary to collect a typical spectrum, can still be implemented to improve data collection or isolate individual signals [19]. More importantly, it is extremely easy to implement and thus we expect our approach will facilitate the use of 2D electronic spectroscopy in numerous research groups.

## 2. Methods

The broad-band ultrashort laser source used in these experiments has been described elsewhere ( $\sim 800$  nm  $\pm$  17 nm;  $\sim 50$  fs temporal FWHM; 1 KHz;  $\sim 900$   $\mu$ J/pulse) [20]. The ‘pump’ portion of the pulse train was coupled into a home-built 4f zero-dispersion pulse shaper. A pixilated dual-layer computer-controlled spatial light modulator (SLM) (CRI Inc; SLM-640) was placed at the Fourier plane of the pulse shaper and calibrated with in-house procedures. Though our SLM has 640 individually addressable pixels, only 130 are used to span the laser spectrum. Phase and amplitude functions applied to the SLM mask produced variably spaced, collinear pulse pairs. The resulting shaped beam (350 nJ/pulse) was focused with a 300 mm lens into a sealed Pyrex one-inch path length Rb gas cell with  $\sim 20$  mTorr of He buffer gas (Triad Technology, Inc.). The cell was heated to  $\sim 135 \pm 2^\circ\text{C}$  to increase the Rb vapor pressure.

The ‘probe’ laser beam was directed onto a computer-driven translation stage providing experimental control of the population time ( $t_2$ ). Approximately 15 nJ/pulse was focused with a 100 mm lens into the sample at a small angle ( $\sim 5^\circ$ ) with respect to the ‘pump’ pulse pair. The signal propagated collinearly with the probe beam and was dispersed with a 1200 g/mm grating in a commercial spectrometer (Acton; Spectrapro 2300i). The dispersed signal was collected on a 1024 pixel photo diode line camera (Spectronic Devices, Ltd; S3904-1024) synchronized with the pulse train, and data were recorded with programs written in house using Labview. Spectra were collected with and without the pump beam and the change in absorption calculated ( $\Delta A = A_{\text{pump off}} - A_{\text{pump on}}$ ). The 2D spectra are generated by Fourier transforming the data as a function of  $t_1$ , as is explained in more detail below.

## 3. Results

To demonstrate our method, we have collected 2D-E spectra of atomic rubidium vapor. Rb vapor has atomic transitions at 794.76 ( $5P_{1/2} \leftarrow 5S_{1/2}$ ) and 780.03 nm ( $5P_{3/2} \leftarrow 5S_{1/2}$ ) and has been used to test other 2D-E methodologies since it has very narrow linewidths [14, 15, 21].

Shown in Fig. 2 is the signal measured at 780 nm as a function of the  $t_1$  delay, incremented in 1 fs intervals with the pulse shaper by stepping the  $E_1$  pulse backwards in time. The signal oscillates with a period of  $\sim 2.6$  fs (see inset), which is set by the transition frequencies. These fast oscillations sit on a background that oscillates with a period of  $\sim 140$  fs, which corresponds to the difference frequency between the 795 and 780 nm transitions. This slow oscillation stems from the transient absorption signal from the first excitation pulse that is being incremented during the experiment and is measured in a standard pump-probe experiment. If desired, it can be straightforwardly removed from the data by phase cycling during the experiment. A similar oscillation is seen for the 795 nm signal.

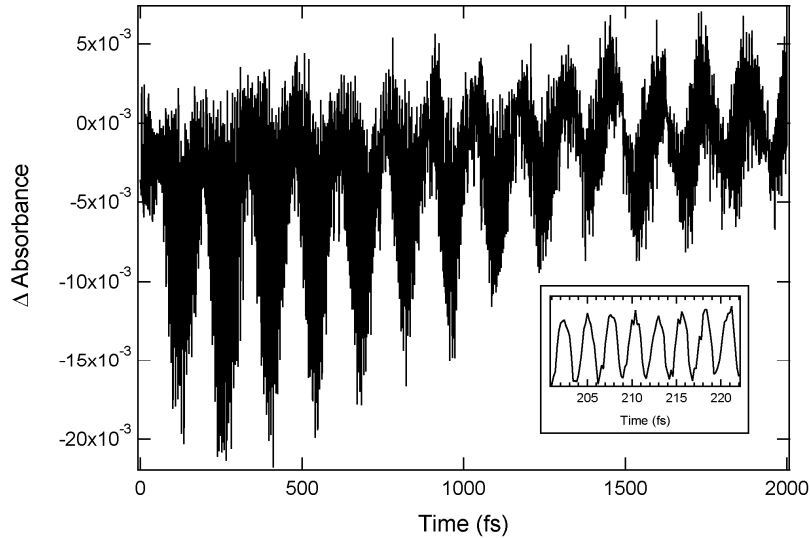


Fig. 2. Time domain data collected at  $\lambda_{\text{probe}} = 780$  nm and  $t_2 = 1.0$  ps. Fast oscillations of the signal (see inset) are superimposed on slow modulation of transient absorption signal.

2D-E spectra are generated by Fourier transforming the time-domain data along  $t_1$  to give  $\omega_1$  (referred to as  $\omega_{\text{pump}}$ ). The spectrometer optically Fourier transforms the signal along  $t_3$  to give  $\omega_3$  ( $\omega_{\text{probe}}$ ). The real part of the 2D-E spectrum is shown in Fig. 3 and exhibits diagonal peaks and cross peaks as expected. The diagonal peaks appear at  $\lambda_{\text{pump}} = \lambda_{\text{probe}} = 780$  and 795 nm ( $\lambda_{\text{pump/probe}} = 2\pi c / \omega_{\text{pump/probe}}$ ) and are created by combinations of pulse interactions (Louvillie pathways) that sample only one of the two transitions [22]. The cross peaks correlate the two diagonal peaks and are created by pathways that sample both fundamental transitions. The intensities are controlled by the transition strengths and the spectrum of the laser pulses. Shown in Fig. 3(b) are both the real and imaginary parts for the diagonal peak at  $\lambda_{\text{pump}} = \lambda_{\text{probe}} = 780$  nm shown in an expanded plot. Well-shaped lineshapes are observed, indicating that the shaper can very accurately step the delay time. Inaccuracies lead to distorted spectra [3]. The linewidths differ along  $\lambda_{\text{pump}}$  and  $\lambda_{\text{probe}}$ , which is to be expected under our experimental conditions. The width of the peaks along the  $\lambda_{\text{probe}}$  axis is determined by the Doppler broadened natural linewidth of the atomic absorption transition ( $\sim 0.001$  nm) convoluted with the spectrometer resolution ( $\sim 0.65$  nm). The width along the  $\lambda_1$  axis is given by the natural linewidth convoluted by the spectral resolution of the Fourier transform,  $1/t_1^{\text{max}}$  where  $t_1^{\text{max}}$  is the largest  $t_1$  delay. For the spectra shown in Fig. 3, we have also convoluted with a cosine window function which decays to zero at 2 ps that further broadens the peak along  $\omega_1$ . This convolution is necessary to avoid signal artifacts and is described in more detail in the Discussion section below.

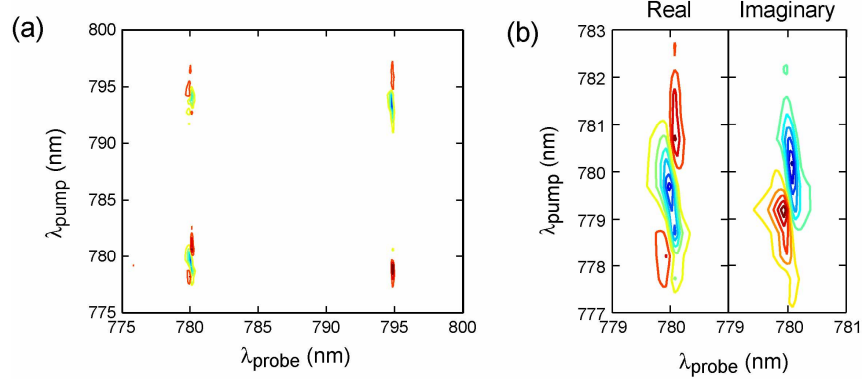


Fig. 3. (color) (a) 2D spectrum of Rb vapor. (b) Detail of the peak at  $\lambda_{\text{pump}} = \lambda_{\text{probe}} = 780$  nm.

Phase stable pulses are critical to the implementation of 2D-E spectroscopy. We measured the phase stability of the pulse pair generated by the shaper. To accomplish this measurement, we scanned  $t_1=200$  to 224 fs in 0.2 fs steps every 21 minutes over the course of 35 hours. The time-domain data were then Fourier transformed to determine the phase angle. Shown in Fig. 4 is the measured phase over the course of 35 hours. From this plot, we calculate that the phase stability is  $\lambda/67$ , which is more than sufficient to generate high quality 2D-E spectra. This number compares to phase drift of  $\lambda/100$  typical of diffractive optics and  $\lambda/250$  with HeNe interferometry; measurements made over the course of  $\sim 5$  hours [4, 5, 7].

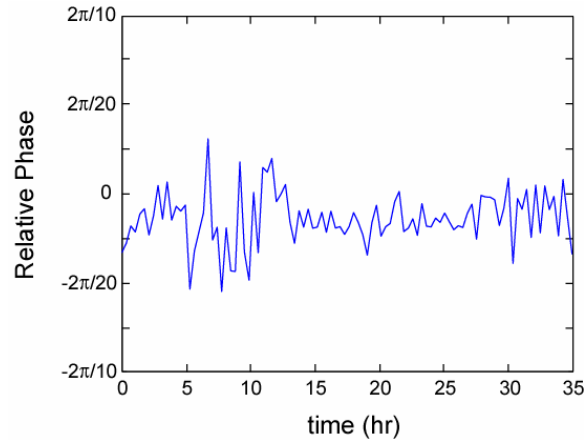


Fig. 4. Phase stability as measured over 35 hours by repeatedly scanning the signal from  $t_1=200 - 220$  fs. Phase drift was measured to be  $\lambda/67$ .

#### 4. Discussion

2D-E spectroscopy is at least a 3rd-order technique, meaning that at least three interactions are required between the pulse sequence and the sample to generate the signal field [22]. If each pulse in the sequence interacts with the sample just once, then a minimum of three pulses are necessary. In our beam geometry, the shaped pump beam interacts with the sample twice and the probe pulse once. The probe pulse also serves to heterodyne the emitted field for phase sensitive detection. The resulting heterodyned signal is Fourier transformed by the spectrometer and collected in the frequency domain. The measured signal can be written as

$$S(t_1, t_2, \omega_{\text{probe}}) = \sum_n \left| \left( R_n(t_1, t_2, t_3) \otimes E_1 \otimes E_2 \otimes E_{\text{probe}} + E_{\text{probe}} \right) e^{-i\omega_{\text{probe}} t} \right|^2 \quad (1)$$

where  $E_1$ ,  $E_2$ , and  $E_{probe}$  are the three necessary electric fields,  $R_n(t_1, t_2, t_3)$  represents the  $n$  orientational and molecular responses of the system, and  $\otimes$  represent convolutions of the electric fields with  $R_n(t_1, t_2, t_3)$ . The 2D-E spectrum is generated by Fourier transforming the signal along  $t_1$  via

$$S(\omega_{pump}, t_2, \omega_{probe}) = \int S(t_1, t_2, \omega_{probe}) e^{-i\omega_{pump}t_1} dt_1 \quad (2)$$

The molecular response is a sum of so-called rephasing, non-rephasing, and two-quantum signals

$$R_n(t_1, t_2, t_3) = R_n^{rephase}(t_1, t_2, t_3) + R_n^{nonrephase}(t_1, t_2, t_3) + R_n^{two-quantum}(t_1, t_2, t_3) \quad (3)$$

where each term in the summation corresponds to a different Feynman pathway that creates a peak in the 2D-E spectrum. These terms contain processes that are commonly referred to as ground state bleaching, stimulated emission, and excited state absorption. To generate absorptive spectra,  $R_n^{rephase}$  and  $R_n^{nonrephase}$  must be measured, phased and added [18].

Spectra collected using  $R_n^{two-quantum}(t_1, t_2, t_3)$  has certain advantages associated with measuring couplings, but is not as often used as  $R_n^{rephase}(t_1, t_2, t_3) + R_n^{nonrephase}(t_1, t_2, t_3)$  because higher-order pulse sequences are needed to generate absorptive spectra [23-25]. In the partially collinear beam geometry,  $R_n^{two-quantum}(t_1, t_2, t_3)$  is only emitted when the probe beam interacts with the sample before the pump beam and thus can be discriminated against by setting  $t_2$  larger than the pulse widths.

Measuring the spectra in this partly collinear geometry alleviates many experimental difficulties associated with both the fully collinear pulse sequence method and the traditional 4-beam setup. In fully collinear geometries where the  $E_{probe}$  pulse is collinear with the  $E_1$  and  $E_2$  pulses, all three responses are generated in-line with the excitation pulses. Thus, unless the excitation pulses are extremely weak, a square-law detector will saturate at low signal levels. This is why fluorescence has been used previously. In the 4-beam setup, all 4 pulses traverse different optical paths. When three pulses are used that each have a unique wavevector such as in a boxcar configuration, then  $R_n^{rephase}$  and  $R_n^{nonrephase}$  must be measured separately because they appear in spatially distinct directions due to phase matching. Furthermore, it is difficult to precisely set the temporal overlaps in the 4-beam setup and thus the spectra have to be carefully calibrated [5, 12]. In the pump-probe phase matching geometry used in this paper,  $R_n^{rephase}$  and  $R_n^{nonrephase}$  are measured simultaneously because they are emitted in the same direction. Moreover, the time-zeros are perfectly set because  $E_{probe}$  serves as both an excitation and heterodyning pulse and because the  $t_1$  time-delay is set with the pulse shaper. Thus, the measured signal is correctly phased and automatically absorptive in nature.

The trick to implementing 2D-E spectroscopy is to achieve adequate phase stability and accurate time resolution. The shaping method employed here produced phase stable pulses because the pulses are collinear and thus follow the same optical paths. Non-collinear pulses are hard to phase stabilize because the lengths of individual optical paths must not drift more than a fraction of the wavelength. In principle, phase drift could be caused by spatial drift of the 800 nm beam into the shaper, which would change the shaper calibration. If such a drift occurred, it might be compensated for by periodic recalibration [3], although this does not seem necessary since our experiments were done in a typical laboratory setting. The full collinear geometry does have the benefit that all of the pulses will be phase stable rather than just  $E_1$  and  $E_2$ . Pulse shaping also provides the additional benefit that phase cycling can be

easily incorporated into signals. Although we have not utilized this feature here, phase cycling allows the signal to be shifted into the rotating frame for faster data collection [26]. Furthermore, phase cycling can be used to minimize the effects of background noise caused by scattered light, because the frequency of the scatter can be shifted away from the signal frequency [16]. We expect this to be an especially advantageous feature in the visible since short wavelengths scatter easily off sample imperfections.

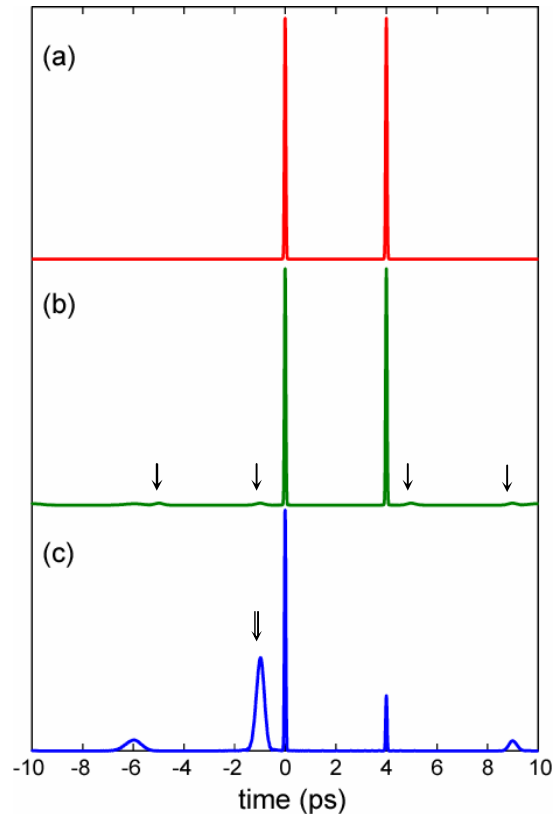


Fig. 5. (a). Simulated pulse pair ( $t_1 = 4$  ps) produced with a perfect shaper. (b). Pulse pair produced with simulated gaps, but otherwise continuous shaping ability. Arrows point to small pulses caused by gaps. (c). Spurious pulses produced as a result of mask pixilation. The double arrow points to a spurious peak that interferes with the signal for  $t_1 > 2$  ps.

For this initial demonstration we chose to use a spatial light modulator (SLM) because it is the most widely used pulse shaping device. However, as has been nicely discussed in the literature, the pixilation of the SLM causes inaccuracies in the pulse pairs [27]. SLMs have an array of independently adjustable liquid crystals separated by small gaps that are not directly controlled by electrodes. Shown in Fig. 5(a) is a simulation of a pulse pair ( $t_1 = 4$  ps) created by a perfect pulse shaper without pixels or gaps. The pulses in the pair are nicely shaped and tail to zero smoothly. Shown in Fig. 5(b) is a simulation of a shaper without pixels, but with 2  $\mu\text{m}$  gaps spaced every 100  $\mu\text{m}$ , the spacing of our SLM. The gaps produce additional pulses, but their effects on the spectra are negligible as they contribute less than 0.01% to the integrated intensity. However, the pixilation of the SLM produces spurious pulses that can influence the experiment. Shown in Fig. 5(c) is a simulation of the shaped pulse using our SLM pixel resolution of 0.428 nm (and no gaps). The SLM pixilation causes spurious peaks at  $\sim 5$  ps intervals (marked with arrows in Fig. 5(c)) relative to the second excitation pulse. The position and intensities of these pulse track with  $t_1$ . In fact, under our simulated conditions, the spurious pulse marked with the double arrow becomes larger than the desired



excitation pulse at 4 ps. FROG measurements confirmed the presence of the largest spurious peak to within 100 fs of where it was predicted by simulation [28].

These spurious peaks have two consequences for 2D-E experiments. First, to compensate for the intensity variation in the excitation pulse, we scale the signal to the peak intensities of the excitation pulses since the signal strength is linearly related to the electric field strength (Eq. (1)). Second, the spurious pulses set the maximum delay that can be used in the experiments. For this reason, we have multiplied the time-domain data with a window function along  $t_1$  that drops to zero by 2 ps, thus limiting the contribution from the spurious peaks to less than 5% of the overall signal intensity. Acoustooptic modulators may be preferable to SLMs because they do not have explicit pixels [27]. However, we expect 128 and 640 pixel LCMs like the one used here will be useful for most condensed phase samples where the signal usually decays within  $\sim 200$ -1000 fs, and thus the maximum time delay necessary can be easily reached without interference from spurious peaks.

## Conclusions

In this paper, we introduce a simple way of implementing 2D-E spectroscopy. By using a pulse shaper to generate collinear pulse pairs, spectra can be collected using a simple pump-probe beam geometry rather than with four individual optical paths in a four-wave mixing geometry. Furthermore, absorptive spectra are automatically generated and perfectly phased, eliminating the need for complicated and potentially inaccurate phase calibrations. Since both the rephasing and non-rephasing spectra are collected simultaneously, data acquisition is also faster. Jonas and coworkers pointed out a number of years ago that both the rephasing and non-rephasing spectra would be collected together in a partly collinear beam geometry [17], but the real advantage comes about when the pulse pair is generated using a shaper, because then high phase stability is achieved, the spectra need not be phase calibrated and phase cycling can be easily implemented. There are still situations where fully collinear geometries might be preferred, such as for pulse sequences where all the beams need to be phase stable. The signal strength of a 4-wave mixing geometry might also be better than the partially collinear geometry since the intensity of the local oscillator is easily adjusted independent from the third excitation pulse [17]. Nonetheless, the simple fact that 2D-E spectroscopy is considerably easier to implement with pulse shaping makes the field much more experimentally accessible. There are probably hundreds of research groups across the world that currently own a pulse shaper suitable to perform 2D-E spectroscopy. We also anticipate the natural combination of this 2D-E methodology with quantum control scenarios utilizing femtosecond pulse shapers to interrogate control mechanisms [20, 29-34].

## Acknowledgments

N.H.D. gratefully acknowledges support from the US Department of Energy (Grant No. DE-FG02-07ER15890).